CrystEngComm

Accepted Manuscript

ROYAL SOCIETY OF CHEMISTRY

www.rsc.org/crystengcomm

Journal Name

RSCPublishing

ARTICLE

Rapid Fabrication of Silver Microplates under an Oxidative Etching Environment Consisting of O_2/Cl^-, NH_4OH/H_2O_2, and H_2O_2

Cite this: DOI: 10.1039/xoxxoooooox

Received ooth January 2012,
Accepted ooth January 2012

DOI: 10.1039/xoxxoooooox

www.rsc.org/

Harnchana Gatemala, Prompong Pienpinijtham, Chuchaat Thammacharoen, Sanong Ekgasit*

Morphologically controlled micro/nanostructures have gained considerable interest as they offer unique properties associated with size, shape, and crystallographic facet. In this paper, we report a simple yet rapid protocol for a large scale synthesis of silver microplates (AgMPls) from silver ammine complex ($[Ag(NH_3)_2]^+$) under an etching environment containing O_2/Cl^-, NH_4OH/H_2O_2, and H_2O_2 capable of dissolving silver crystals except plate structures. H_2O_2 is employed as the sole reducing agent. Chloride ions are essential for creating etching environment capable of selective dissolution of single and multiply twinned crystals, while leaving plate structures unaffected. Without chloride ions, H_2O_2 reduces $[Ag(NH_3)_2]^+$ complex to silver microparticles containing truncated cubes, icosahedra, pentagonal rods, and plate microstructures with icosahedra as the major product. The developed protocol enables an environmental friendly fabrication of highly pure AgMPls and AgMPs directly from AgCl precipitate.

Introduction

In the past decade, morphology-controlled synthesis has become an important means for the fabrication of functional materials with desired properties as the nano-enable properties could be efficiently controlled through the size and shape manipulation. Functional micro/nanostructure of silver has attached much attention as it offers potential applications in catalyst, electronic device, sensor, and medical device fabrications. Complex structures including nanocubes,[1] nanoplates,[2-4] nanorods,[5] nanowires,[6, 7] and branched microcrystals[8] were successfully synthesized. Reviews on the synthesis and characterization of silver nanoplates have recently been published.[9-12] The plate like nanostructure with large contact area has shown potential application in the fabrication of solar cell with high photocurrent.[13]

The morphology of silver micro/nanostructures can be tuned through seed selection and growth process.[12, 14, 15] The morphology of seed particles is crucial for the structural controlled synthesis as it dictates the final products. The single crystal seed grows to cube, octahedron, tetrahedron, and rectangular bar. The singly twinned seed grows to right bipyramid and beam. The multiply twinned seed grows to decahedron, icosahedron and pentagonal rod. The plate with stacking faults seed grows to hexagonal and triangular plate. Oxidative etching has been employed for selective preservation or selective elimination of certain crystallographic structures. For example, Cl^-/O_2 dissolves singly and multiply twinned seeds,[5, 16-18] halide ion etches Ag{110} facets,[18] NH_4OH/H_2O_2 etches single crystal seeds containing Ag{100} facets,[19, 20] while H_2O_2 etches all silver structures.[21] Surface blocking was also practiced in shape-controlled synthesis. Several organic capping agents such as citrate, cetyltrimethylammonium bromide (CTAB), poly(vinyl pyrrolidone) (PVP) and inorganic capping agents such as halide ions, cyanide ion, and thiol were used for selective protection of certain facets while promoting growth on the non-protected facets.[22-28]

The efficient catalytic decomposition of hydrogen peroxide (H_2O_2) by silver metal was well-documented.[29-31] The decomposition of H_2O_2 on silver metal at high concentration is extremely violent with a releasing of intense heat, water vapor, and oxygen gas. H_2O_2 has been employed as an efficient etchant and a seed-selecting agent for the fabrication of silver nanostructures.[21, 32-34] Although H_2O_2 is well-known as a strong oxidizing agent, it is an efficient reducing agent under an alkaline condition.[8, 34-37] There are few reports exploiting the reducing capability of H_2O_2 for the fabrication of silver micro/nanostructures. Silver nanosheets and 3D flowerlike silver microstructures were fabricated by H_2O_2 reduction of Ag^+ and $[Ag(NH_3)_2]^+$.[8, 36] Recently, a direct synthesis of silver microdisk on a plastic substrate by H_2O_2 reduction was demonstrated.[37]

This paper reveals a simple yet efficient approach for the production of silver microplates *via* H_2O_2 reduction of

$[Ag(NH_3)_2]^+$ complex under an influence of Cl^-. For the first time, we demonstrated a fabrication of silver microplates under an etching environment containing O_2/Cl^-, NH_4OH/H_2O_2, and H_2O_2. Under such environment, the survival of plate structures were promoted by chloride passivation of the dominated Ag{111} facets while truncated cubes, icosahedra, and pentagonal rods with Ag{100} envelopes were selectively destroyed. This method has several advantages including: (1) simple and rapid as the reaction is completed within 1 h, (2) operated under an ambient condition with high concentration of silver ion, (3) employed environmentally friendly reducing agent without using any capping agent or surfactant, and (4) ease separation of products. We also demonstrated a direct preparation of AgMPs and AgMPls from wasted silver chloride precipitates using the developed protocol.

Experimental Section

Chemicals: Silver nitrate ($AgNO_3$, purity≥99.8%), sodium chloride (NaCl, purity≥99%), nitric acid (HNO_3, 65% w/v), ammonium hydroxide solution (NH_4OH, 25% w/w), and hydrogen peroxide solution (H_2O_2, 30% w/w) were purchased from Merck®. Poly(vinyl pyrrolidone) (PVP, $M_w \approx 360{,}000$) was purchased from Aldrich. All chemicals were used as received. Deionized (DI) water was used as a solvent. Prior to use, all glassware and magnetic bars were thoroughly cleaned with detergent, rinsed with DI water, rinsed with 6 M nitric acid, and thoroughly rinsed again with DI water.

Reducing capability of H_2O_2: To demonstrate the reducing capability of H_2O_2 under an alkaline condition, silver microparticles (AgMPs) were synthesized from colorless silver ammine complex ($[Ag(NH_3)_2]^+$). Briefly, a clear solution of $[Ag(NH_3)_2]^+$ complex (~pH 10) was prepared by mixing $AgNO_3$ solution (1 M, 1 mL) with an NH_4OH (5.3 M, 1.7 mL) and PVP (5% w/v, 10 mL). The total volume was adjusted to 97.7 mL by DI water. As H_2O_2 (30% w/w, 2.3 mL) was added into the solution, the reduction of the complex to metallic silver could be noticed *via* the evolution of oxygen bubbles with an instant development of light brown silver colloid. The precipitated AgMPs were collected and cleaned with DI water. Under this condition, the concentration of $AgNO_3$, NH_4OH, H_2O_2 and PVP were 0.01 M, 0.09 M, 0.22 M, and 0.5% w/v respectively.

Synthesis of silver microplates (AgMPls): AgMPls were selectively synthesized *via* the reduction of $[Ag(NH_3)_2]^+$ with a presence of Cl^- using H_2O_2 as a reducing agent. Briefly, a colloid of AgCl nanoparticles (AgClNPs) was prepared by a rapid injection of NaCl solution (0.1 M, 4 mL) into a solution of $AgNO_3$ (1 M, 1 mL) and PVP (5% w/v, 10 mL) under a vigorous stir. A milky white colloid of AgClNPs spontaneously developed. The total volume was adjusted to 96 mL by DI water. The colloid was further stirred for 5 min before an addition of NH_4OH solution (5.3 M, 1.7 mL). The colloid became less opaque due to a partial dissolution of AgClNPs with a formation of a water soluble $[Ag(NH_3)_2]^+$ complex (Equation 1). To induce a formation of AgMPls, H_2O_2 solution (30% w/w, 2.3 mL) was quickly injected into the colloid. The milky white colloid briefly turned light brown before becoming sparkling glitter within 2 min due to the formation of AgMPls. The development of AgMPls and the progress of the reaction could be noticed by an evolution of oxygen bubbles (Equation 2). [38] The colloid became intense glittering as the reaction proceeded while the white AgClNPs were disappeared. The colloid was further stirred for 1 h to ensure a complete reaction. The shiny silver precipitates were collected and washed 5 times with DI water. Under the standard condition, the concentration of NaCl, NH_4OH, H_2O_2, $AgNO_3$, PVP were 0.004, 0.09, 0.22, 0.01 M, and 0.5% w/v respectively. To investigate the influence of Cl^-, NH_4OH, H_2O_2, Ag^+, and PVP on the morphology of AgMPs, their final concentrations were systematically manipulated within the range of 0–50 mM, 0–0.45 M, 0–0.88 M, 5–40 mM, and 0–2% w/v respectively.

$$AgCl + 2NH_4OH \rightleftharpoons [Ag(NH_3)_2]^+ + Cl^- + 2H_2O \quad (1)$$

$$2[Ag(NH_3)_2]^+ + H_2O_2 \longrightarrow 2Ag + 4NH_3 + 2H_2O + 1/2O_2 \; ; E^0_{cell} = 0.227\ V \quad (2)$$

Structural Investigation: Morphology (size and shape) of the AgMPs and AgMPls was recorded by a scanning electron microscope (SEM, JEOL JSM-6510A) operating at 20 kV under a high vacuum mode with a secondary electron image (SEI) detector. A built-in energy dispersive X-ray spectrometer (EDS) was employed for monitoring elemental compositions of the AgMPls. The X-ray diffraction (XRD) patterns were collected by an X-ray diffractometer (Philips PW3710) operated at room temperature with a scanning rate of 0.02 deg/min, using Cu K_α irradiation (40 kV, 30 mA). The diffractograms were recorded in the 30°–80° region with a 0.2° resolution. X-ray photoelectron spectra (XPS) were performed on an AXIS ULTRA (Kratos Analytical, England) using Al K_α X-rays (1486.6 eV) as the exciting source. The charging calibration was performed by referring the C1s to the binding energy at 285 eV. The XPS data analysis was conducted with standard ESCA-300 software package.

Results and Discussion

Figure 1 shows an SEM micrograph of the silver microcrystals synthesized by the H_2O_2 reduction of $[Ag(NH_3)_2]^+$ without Cl^-. The microcrystals consisted of truncated cubes, icosahedra, pentagonal rods, hexagonal plates, and irregular particles. According to a detailed structural investigation (Figure S1), the irregular-shaped particles were, in fact, the under developed icosahedra. Based on a statistical analysis of 500 particles from non-

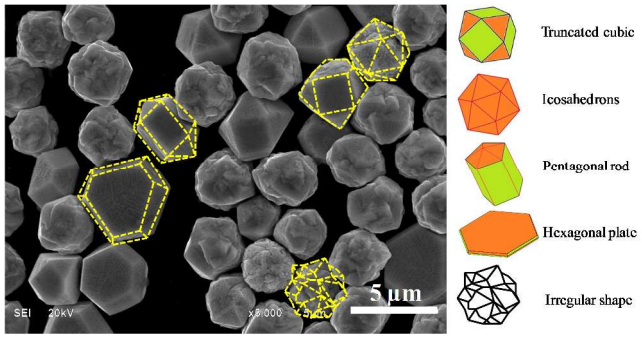

Figure 1. An SEM micrograph of AgMPs synthesized by H_2O_2 reduction of $[Ag(NH_3)_2]^+$. The orange and green surfaces indicated {111} and {100} facets, respectively. The experimental condition are $[AgNO_3]$ = 10 mM, $[NH_4OH]$ = 0.09 M, $[H_2O_2]$ = 0.22 M, and [PVP] = 0.5% w/v.

overlapping SEM micrographs, the as-synthesized AgMPs consisted of 10.4% truncated cubes, 82.1% icosahedra and pentagonal rods, and 7.5% hexagonal plates (Figure S2A). The structural distribution confirmed that the multiply twinned crystals were the most thermodynamically favorable structures as they grown into icosahedra and pentagonal rod.[5, 14, 39] The multiply twinned are known to favorably developed at high concentration of gold and silver ions. [39] H_2O_2 is known to etch silver nanoparticle with a selective preservation of Ag{111} facets.[21] NH_3, on the other hand, selectively passivate and prohibit etching of Ag{111} facets.[6] As a result, crystals with dominated Ag{111} facets (i.e., icosahedra) could withstand the oxidative etching of H_2O_2 and NH_4OH.

The isolated AgMPs also suggested that PVP plays an important role on facilitating particles growth as well as preventing aggregation. The well-separated particles with uniform size of 3–4 μm suggest a non-overlapping nucleation and growth period enabled by a sufficient stabilization by PVP and surface passivation by NH_3.[6]

Due to the positive electrochemical potentials of Equations 2, $[Ag(NH_3)_2]^+$ can be reduced by H_2O_2.[8, 36, 37] With the presence of NH_4OH, $[Ag(NH_3)_2]^+$ instantaneously forms due to the high complex formation constant of NH_3 with Ag^+ (K_f = 1.6x10^7).[40] We hypothesized that $[Ag(NH_3)_2]^+$ functioned as the silver supply for the formation of AgMPs. Under a neutral condition, H_2O_2 efficiently oxidizes silver nanospheres to Ag^+.[41] However, under an alkaline condition, H_2O_2 does not etch the newly generated seeds with stacking faults while the greater reduction potential compared to the oxidation potential favor the reduction.[34] As a result, silver seeds with stacking faults survived and grew into micrometer size AgMPs even at a relatively high concentration of H_2O_2 (i.e., in Figure 1, $[H_2O_2]/[Ag^+] = 22$).

Selective formation of AgMPls: Since Cl^- with dissolved O_2 is known to selectively etch singly and multiply twinned seed,[5, 16-18] the reduction of $[Ag(NH_3)_2]^+$ by H_2O_2 under the influence of Cl^- was conducted. The addition of Cl^- was expected to work synergically with the *in-situ* generated O_2 from H_2O_2 decomposition as an efficient O_2/Cl^- etchant. Figure 2 shows structural evolution of AgMPs under the influence of Cl^-. Surprisingly, even at a very low concentration of Cl^- (0.05 mM, Figure 2B), large icosahedra disappeared with a development of silver nanoplates (AgNPls). According to a statistical calculation of more than 500 particles from non-repeating SEM micrographs (Figure S2), the products consist of 2.5% small truncated cubes (average size of 1 μm), 76.4% small icosahedra (average size of 1 μm), and 21.1% microplates (average bisector length of 3 μm). When the concentration of Cl^- ion was increased, the AgNPls became larger and thicker (average bisector length of 9 μm and average thickness of 300 nm). The truncated cubes and the icosahedra disappeared as the concentration of Cl^- was increased to 4 mM (Figures 2E, S2, and S3). However, when the concentration of Cl^- was greater than 10 mM, the AgMPls were not obtained since all $[Ag(NH_3)_2]^+$ was precipitated as AgCl (Figures 2H and 2I). The solid AgCl is non-soluble in the reaction media due to the low concentration of NH_4OH. The H_2O_2 reduction of solid AgCl to metallic silver cannot be achieved unless more NH_4OH is added in order to generate the water soluble $[Ag(NH_3)_2]^+$. The AgMPls in Figure 2E were highly pure silver (99.5%) as confirmed by EDS and XRD data (Figure S4 and S5A). According to EDS data, a trace amount of chloride indicated a formation of thin AgCl film on the basal planes.[26-28] The thin AgCl film can be removed by washing with 0.1 M NH_4OH solution (Figure S4). The XRD data in Figure S5B show that the intensity ratios of (111) and (200) peaks increase with an increasing of Cl^- concentration which correspond to the higher number of AgMPls population. The silver nanostructures[13, 42] similar to those in Figures 2C–2F have been employed for electronic device fabrication and substrate for thin film solar cell. The smooth surface with large contacted area enable a prolong service lifetime in conductive ink and high photocurrent enhancement in thin film solar cells.[13]

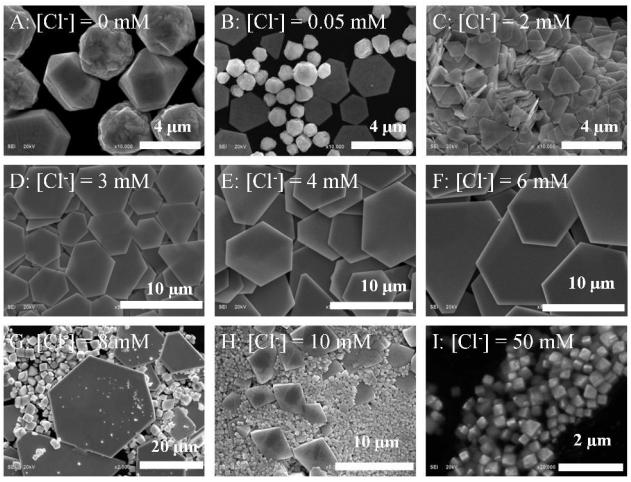

Figure 2. SEM micrographs show AgMPls synthesized by H_2O_2 reduction of $[Ag(NH_3)_2]^+$ under the influence of $[Cl^-]$: (A) 0, (B) 0.05, (C) 2, (D) 3, (E) 4, (F) 6, (G) 8, (H) 10, and (I) 50 mM. The experimental condition are $[AgNO_3]$ = 10 mM, $[H_2O_2]$ = 220 mM, $[NH_4OH]$ = 90 mM, [PVP] = 0.5% w/v. The Cl^- was introduced in the form of NaCl solution before an addition of H_2O_2.

The selective dissolution of multiply twinned and single crystal particles by O_2/Cl^- [5, 16-18] and NH_4OH/H_2O_2 [19, 20] has been reported. In our case, the O_2 gas was *in-situ* generated by the H_2O_2 oxidation (Equation 2), the auto-decomposition of H_2O_2 over silver surface,[29] and the auto-decomposition of H_2O_2 under alkaline condition.[43] An addition of Cl^-, thus, induced a formation of O_2/Cl^- etchant which capable of dissolving multiply twinned and single crystals while promoting the survival of AgMPls by Cl^--passivation.

To gain an insight understanding on the selective formation of AgMPls under the etching environment, a systematic investigation was performed. Figure 3 shows the effect of NH_4OH, Ag^+, H_2O_2, and PVP on the morphology of silver microstructures. In an acidic medium (pH<5) without NH_4OH (Figure 3A1), H_2O_2 cannot reduce Ag^+ or AgCl to metallic sliver at any concentration.[34] The reducing efficiency of H_2O_2 could be enhanced by increasing pH either by NH_4OH or NaOH[34, 35, 44] (Figure S6). When a minute amount of NH_4OH was added (Figure 3A2), AgNPls was formed. However, residual AgCl particles remained due to an incomplete reduction at a near neutral pH. The formation of AgNPls suggested that a seed selection process was initiated with an introduction of NH_4OH. Quasi-sphere AgMPs obtained when the reduction was conducted under NaOH (Figure S6). At NH_4OH concentration of 0.09–0.18 M, AgMPls (3–40 μm lateral size and 0.2–1.1μm thickness, Figures 3A3–3A5) were obtained. The reduction was very

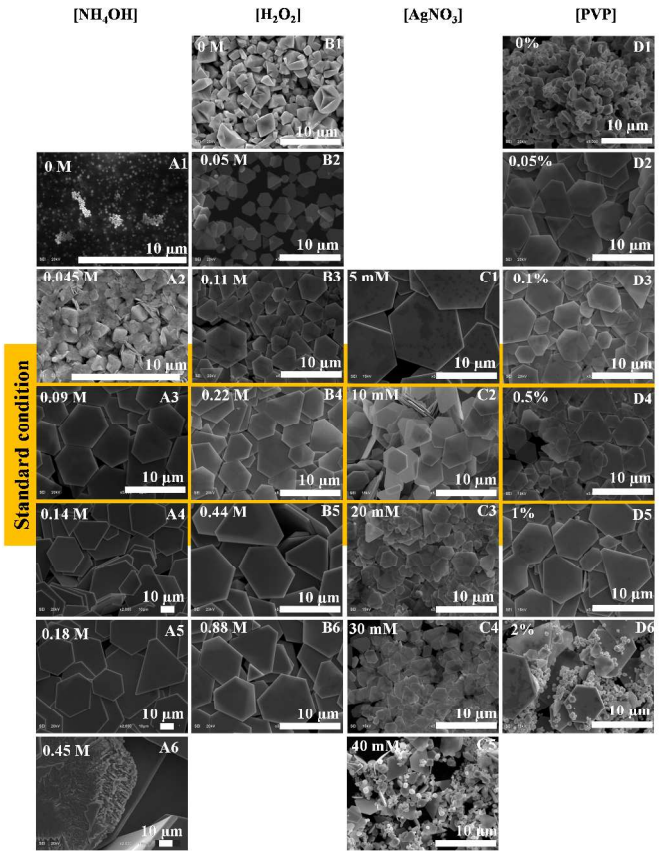

Figure 3. SEM micrographs show morphological change of AgMPs induced by the concentration of the reactants: (A) NH_4OH, (B) H_2O_2, (C) $AgNO_3$, and (D) PVP. The concentration is indicated in the figure. The scale bars indicate 10 µm.

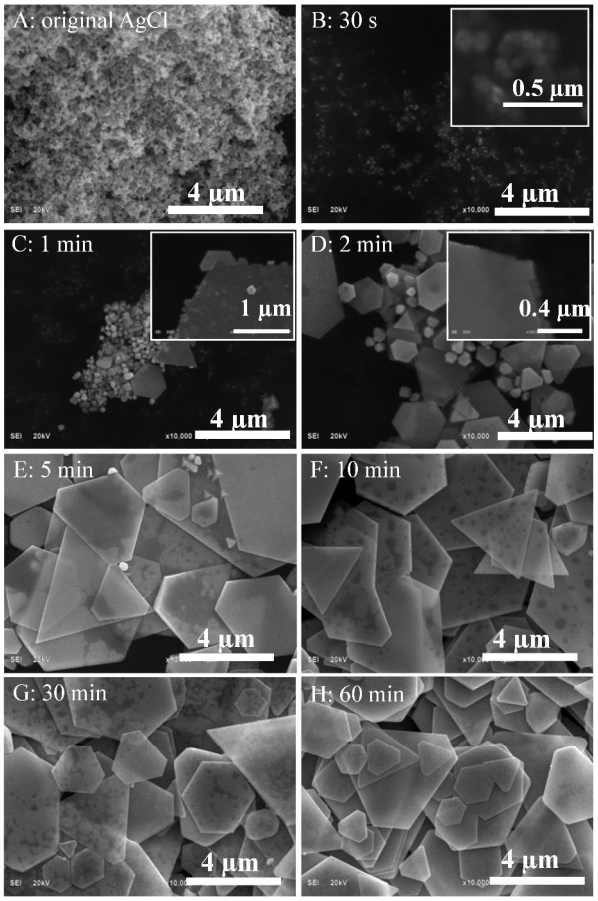

Figure 4. The time dependent SEM micrographs show evolution of AgMPls synthesized under the same condition as that of Figure 2F. The time was recorded after an injection of H_2O_2 reducing agent. Scale bars indicate 4 µm.

rapid as AgMPls formed and precipitated within 1 min after an addition of H_2O_2. At a relatively high NH_4OH concentration of 0.45 M, the reduction was incomplete with a formation of large AgMPls having a broad size distribution (10–120 µm lateral size). H_2O_2 was also rapidly exhausted due to the alkaline-induced decomposition and auto-decomposition on silver surface.[29, 43]

Figure 3B1 confirmed that H_2O_2 is the sole reducing agent as AgCl crystals were obtained in the absence of H_2O_2. By adding a minute amount of H_2O_2 (0.05 M, Figure 3B2), AgNPls formed with a remaining solid AgCl. Under the employed condition, 0.11 M H_2O_2 was enough to completely convert $[Ag(NH_3)_2]^+$ complex to AgMPls (Figures 3B3-3B6). The plate size was increased from 4 µm to 23 µm while the plate thickness was increased from ~400 nm to 700 nm when H_2O_2 concentration was increased from 0.11 M (Figure 3B3) to 0.88 M (Figure 3B6). The sharp edges with smooth basal planes suggested that AgMPls tolerated the oxidative etching at high concentration of H_2O_2.

Figure 3C shows the influence of $AgNO_3$ concentration while the ratio of $[H_2O_2]$:$[Ag^+]$ was kept constant at 22. Large AgMPls were obtained at low concentration of $AgNO_3$ (5 mM, Figure 3C1). The AgMPls systematically transformed to AgNPls as the $AgNO_3$ concentration was increased. The lateral size was decreased from 15 µm to 3 µm while the thickness was decreased from 300 nm to 80 nm as the $AgNO_3$ concentration was increased from 5 mM to 30 mM (Figures 3C2–3C4). However, at an extremely high concentration of $AgNO_3$ (40 mM, Figure 3C5), a mixture of AgMPls (lateral size of 4 µm and thickness of 200 nm) and microsphere (particle size of ~1–2 µm) was obtained. The structural change was due to: (1) a large number of seed generated under a high concentration of H_2O_2, (2) a rapid growth under an increased concentration of $AgNO_3$, and (3) an insufficient etching under a constant Cl^- concentration of 4 mM. Although O_2/Cl^- is known to efficiently etch multiply twinned seed,[5, 16-18] silver microspheres in Figure 3B5 survived due to a low concentration of Cl^-. A significant aggregation was also observed at high concentration of $AgNO_3$ (40 mM, Figure 3C5) due to an insufficient stabilization of PVP (0.5% w/v).

From the previous investigations (Figures 3A–3C), PVP (0.5% w/v) functions as a good stabilizer preventing aggregation of AgMPls and AgNPls. PVP is known to preferentially adsorb on Ag{100} facet.[45-47] Without an addition of PVP (Figure 3D1), only aggregated AgMPs (1–5 µm) were obtained. Surprisingly, an insignificant structural change of AgMPls (lateral size of ~6 µm and thickness of 150 nm) was observed as the concentration of PVP was increased from 0.05 to 1 % w/v. This minor structural variation suggested that PVP functioned only as a stabilizer without any interference on nucleation and growth of

AgMPls (Figures 3D2–D5). The expansion of the basal plane was induced by the weaker adsorption of PVP on Ag{100} facets[45-47] with a passivation of NH_3,[6] Cl^-,[22-26] and AgCl[26-28] on Ag{111} facets. These resulted in a greater deposition rate of silver atoms on Ag{100} facet than Ag{111} facet. However, a relatively high concentration of PVP of 2% w/v induced an incomplete reduction as AgCl microparticles (AgClMPs) were the main product with a formation of large AgMPls (lateral size of ~15 µm and thickness of ~300 nm, Figure 3D6). As the concentration of H_2O_2 was kept constant at 220 mM, the formation of AgClMPs indicated an insufficient reduction power of H_2O_2 at high concentration of PVP as it forms stable complex between PVP.[48-51]

Based on the observed phenomena, we believed that the water soluble $[Ag(NH_3)_2]^+$ complex is the sole species being reduced by alkaline peroxide. With the available NH_4OH, all Ag^+ were transformed into the complex.[40, 52] However, when the alkalinity was adjusted by NaOH, quasi-sphere AgMPs (Figure S6) were obtained instead of AgMPls. NH_4OH is one of the key factors for the development of plate shape structures as it imposes the following constraints: (1) NH_4OH decreases the rate of reduction by forming a stable $[Ag(NH_3)_2]^+$ complex with lower E^0 compared to that of Ag^+,[38] and (2) NH_4OH/H_2O_2 selectively etches single crystal particles.[19, 20]

One of the interesting phenomena in this system is the survival and systematic growth of large AgMPls under a highly corrosive environment containing O_2/Cl^-, NH_4OH/H_2O_2, and H_2O_2. Figure 4 shows evolution of AgMPls as the water soluble $[Ag(NH_3)_2]^+$ complex was reduced by H_2O_2 solution. After a 30-s of H_2O_2 injection (Figure 4B), quasi-sphere silver particles (100–200 nm) were generated. At 1-min (Figure 4C), the quasi-sphere developed into silver crystals including truncated cubes, icosahedra, and plates. At 2-min (Figure 4D), those crystals grow into microstructures. Interestingly, the plate structures grow larger in terms of number and size (1–4 µm lateral size) compared to those of icosahedra and truncated cubes (0.6–0.8 µm). At 5-min, the majority of the silver structures are large AgMPls (1–10 µm lateral size) with rough surface (Figure 4E). A few numbers of small icosahedra and truncated cubes (~0.5 µm) were occasionally observed in SEM micrographs. The change in population and morphology indicated a selective dissolution of icosahedra and truncated cubes as those structures completely disappeared after 10-min (Figure 4F). One interesting morphological change of the AgMPls is the increased smoothness of the basal planes after a prolong reaction time, as indicated by SEM micrographs in Figure 4E–4H. AgMPls with flat and smooth surfaces were obtained after 60-min.

Figure 3B6 suggested that the AgMPls were very stable under the extremely high concentration of H_2O_2 (0.88 M). The stability of AgMPls was due to the passivation of Ag{111} by Cl^-,[22-26] and AgCl.[26-28] H_2O_2 and NH_4OH/H_2O_2 selectively destroyed the truncated cubes (single crystal particles),[19, 20] while O_2/Cl^- selectively etched the multiply twinned particles.[5, 16-18] Our results indicated that the O_2/Cl^- also etched the truncated cubes (Figures 2A and 2E).

In Figure 5, we proposed a mechanism explaining the rapid growth of AgMPls under the employed etching environment. As shown in Figure 1, H_2O_2 could reduce water soluble $[Ag(NH_3)_2]^+$ complex into silver crystals. The growths of cubes from single crystal seeds, icosahedra and pentagonal rods from multiply twinned seeds, and hexagonal and triangular plates from seeds with stacking faults were

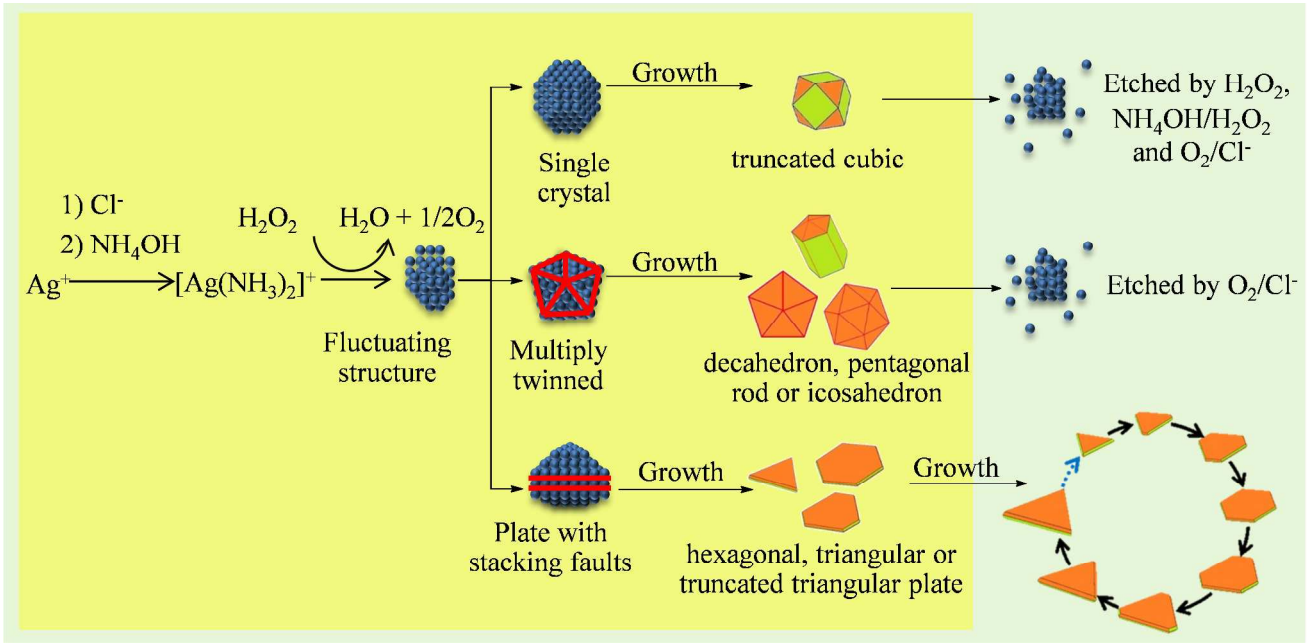

Figure 5. The proposed mechanism on the selective formation of AgMPls under an etching environment containing NH_4OH/H_2O_2, H_2O_2, O_2/Cl^-. The single crystal and multiply twinned crystal were selectively destroyed. The stability of the plate structure was due to the passivation of Ag{111} facets. The green facets indicate Ag{100} while the orange facets indicate Ag{111}.

Journal Name RSCPublishing

ARTICLE

thoroughly explained.[12, 14, 15] An addition of Cl^- initiated an etching environment with selective survival of plate structures. The asymmetric twinned nanoplates bound by Ag{111} planes with alternated Ag{100} and Ag{111} lateral sides were formed.[53, 54] The surface passivation of Ag{111} by Cl^- and AgCl limited the atomic deposition on the basal planes and decreased the rate of thickness growth. The adsorption of Cl^- on the basal planes of AgMPls was confirmed by the EDS and XPS data. The XPS results show that AgCl was adsorbed on the basal planes of as-prepared AgMPls as indicated by the binding energy of Cl 2p at 197.5 and 199.0 eV,[55-58] Figure 6B. To confirm the presence of AgCl, as-prepared AgMPls were washed by 0.1 M NH_4OH. The trace AgCl was completely removed after washing (Figures 6B and S4B). The bare surface of AgMPls was slowly oxidized to Ag_2O after a prolong storage under an ambient condition, as indicated by O 1s at 531.5 eV (Figure 6C).[58-60]

In addition, the adsorption of PVP-Ag^+ complex on Ag{100} facets promotes growth along the lateral side[10, 36, 46, 61-64] (Figure S7). An anisotropic growth due to a faster expansion of Ag{100} compared to that of Ag{111} induces a cyclic structural transformation of triangular, truncated triangular, and hexagonal structure.[53, 54] The growth continued until the $[Ag(NH_3)_2]^+$ complex was depleted.

One of the potential applications of our developed technique is the direct fabrication of AgMPs and AgMPls from AgCl precipitates. The silver wastes were normally digested or leached into Ag^+ before precipitating as solid AgCl for easy separation. The AgCl precipitates were then converted to metallic silver by electrochemical deposition,[65] galvanic replacement,[66] chemical reduction[67] and hydrometallurgical recovery.[68, 69] However, the processes are labor intensive, expensive, and generate more chemical wastes. Due to the 1:1 mole ratio of Ag^+:Cl^- in the precipitated AgCl, the procedure employed in Figure 2H could only partially convert AgCl into metallic silver after a prolong reaction of 15 h (Figure 7A). The inefficient reduction was due to a very slow conversion of AgCl to $[Ag(NH_3)_2]^+$ complex at a relatively low [NH_4OH] of 0.09 M while H_2O_2 cannot reduce solid AgCl to metallic silver. To improve the conversion, NH_4OH concentration was increased to 0.18 M (Figure 7B). Large AgMPls were precipitated when NH_4OH concentration was increased to 0.27 and 0.36 M (Figures 6C and 6D). In the absence of PVP, for comparison, the precipitates contained microplates, truncated cubes, and icosahedra (Figure S8).

Our technique offers a rapid, economic, and environmentally friendly protocol for silver recovery under an ambient condition. It does not create additional chemical waste as H_2O_2 was employed as the sole reducing agent. The main advantages of our developed technique include: (1) high recovery ratio of greater than 95%, (2) easily separated AgMPls precipitates (3) highly pure recovered AgMPls

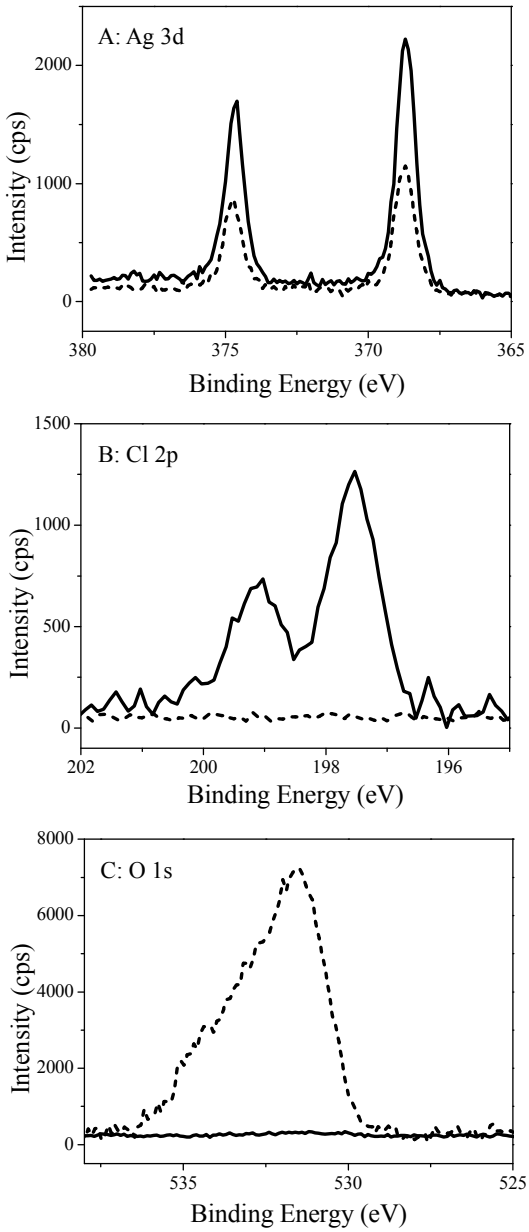

Figure 6. XPS spectra of as-prepared AgMPls (solid line) and 6-month storage AgMPls (dotted line). The as-prepared AgMPls were metallic silver with AgCl passivation as indicated by Ag 3d (A) and Cl 2p (B) spectra. The surface of cleaned AgMPls was oxidized into Ag_2O after a prolong storage as indicated by O 1s spectrum (C).

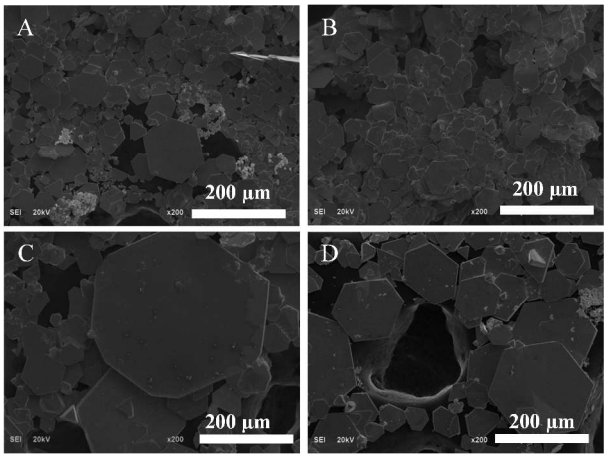

Figure 7. SEM micrographs show AgMPls directly fabricated from solid AgCl using our developed technique. The experimental condition is the same as that of Figure 2H with NH_4OH concentration of (A) 0.09, (B) 0.18, (C) 0.27, and (D) 0.36 M. The scale bars are 200 µm.

(99.99%, Figure S9), (4) tap water or water with Cl^- contamination can be employed instead of DI water, and (5) environmentally friendly process (by-products included O_2, H_2O, and NH_4Cl).

Conclusions

We have developed a simple yet rapid technique for a large scale synthesis of AgMPls from $[Ag(NH_3)_2]^+$ using H_2O_2 as the reducing agent under an etching environment containing O_2/Cl^-, NH_4OH/H_2O_2, and H_2O_2. A trace Cl^- induced an etching environment that only plate structures could withstand as it passivated the Ag{111} facets of the plates. The time dependent SEM investigations confirmed that Cl^- promoted the survival of plate structures while selectively destroyed truncated cubes, icosahedra, and pentagonal rods containing Ag{100} envelops. In the system without Cl^-, etchants capable of structural selectivity does not exist. As a result, H_2O_2 reduction of $[Ag(NH_3)_2]^+$ complex produce silver microparticles including truncated cubic, icosahedral, pentagonal rod, and plate microstructures with icosahedra as the major product. A potential application of the developed protocol for a fabrication of highly pure AgMPls directly from AgCl precipitates has been demonstrated.

Acknowledgements

This research has been supported by the National Research University Project, the Office of Higher Education Commission (WCU-033-AM-57). H. Gatemala is a scholar under the Development and Promotion of Science and Technology Talents (DPST) Project.

Notes and references

Sensor Research Unit, Department of Chemistry, Faculty of Science, Chulalongkorn University 254 Phyathai Road, Patumwan, Bangkok 10330, Thailand
E-mail: sanong.e@chula.ac.th

†Electronic Supplementary Information (ESI) available: SEM, XRD, EDS, and statistical data related to the formation and growth of AgMPls. See DOI: 10.1039/b000000x/

1 X. Xia, J. Zeng, Q. Zhang, C. H. Moran and Y. Xia, *J. Phys. Chem. C*, 2012, **116**, 21647-21656.
2. B. Tang, S. Xu, J. An, B. Zhao and W. Xu, *J. Phys. Chem. C*, 2009, **113**, 7025-7030.
3 J. Yang, Q. Zhang, J. Y. Lee and H.-P. Too, *J. Colloid Interface Sci.*, 2007, **308**, 157-161.
4 Z. Zaheer and Rafiuddin, *Colloids Surf., A*, 2012, **393**, 1-5.
5 B. Wiley, T. Herricks, Y. Sun and Y. Xia, *Nano Lett.*, 2004, **4**, 1733-1739.
6 J. Du, B. Han, Z. Liu, Y. Liu and D. J. Kang, *Cryst. Growth Des.*, 2007, **7**, 900-904.
7 S.-H. Zhang, Z.-Y. Jiang, Z.-X. Xie, X. Xu, R.-B. Huang and L.-S. Zheng, *J. Phys. Chem. B*, 2005, **109**, 9416-9421.
8 H. Chen, E. Kern, C. Ziegler and A. Eychmüller, *J. Phys. Chem. C*, 2009, **113**, 19258-19262.
9 Z. Khan, J. I. Hussain, S. Kumar and A. A. Hashmi, *Colloids Surf., B*, 2011, **86**, 87-92.
10 X. Luo, Z. Li, C. Yuan and Y. Chen, *Mater. Chem. Phys.*, 2011, **128**, 77-82.
11 Y. Xia and N. J. Halas, *MRS Bull.*, 2005, **30**, 338-348.
12 Y. Xia, Y. Xiong, B. Lim and S. E. Skrabalak, *Angew. Chem. Int. Ed.*, 2009, **48**, 60-103.
13 K. R. Catchpole and A. Polman, *Appl. Phys. Lett.*, 2008, **93**, (191113-1)-(191113-3).
14 Y. Xiong and Y. Xia, *Adv. Mater.*, 2007, **19**, 3385-3391.
15 S. Maksimuk, X. Teng and H. Yang, *J. Phys. Chem. C*, 2007, **111**, 14312-14319.
16 S. H. Im, Y. T. Lee, B. Wiley and Y. Xia, *Angew. Chem.*, 2005, **117**, 2192-2195.
17 X. Tang, M. Tsuji, P. Jiang, M. Nishio, S.-M. Jang and S.-H. Yoon, *Colloids Surf., A*, 2009, **338**, 33-39.
18 S. Xu, B. Tang, X. Zheng, J. Zhou, J. An, X. Ning and W. Xu, *Nanotechnology*, 2009, **20**, 1-7.
19 C. M. Cobley, M. Rycenga, F. Zhou, Z.-Y. Li and Y. Xia, *J. Phys. Chem. C*, 2009, **113**, 16975-16982.
20 M. J. Mulvihill, X. Y. Ling, J. Henzie and P. Yang, *J. Am. Chem. Soc.*, 2009, **132**, 268-274.
21 M. Tsuji, S. Gomi, Y. Maeda, M. Matsunaga, S. Hikino, K. Uto, T. Tsuji and H. Kawazumi, *Langmuir*, 2012, **28**, 8845-8861.
22 G. Aloisi, A. M. Funtikov and T. Will, *J. Electroanal. Chem.*, 1994, **370**, 297-300.
23 G. Beltramo and E. Santos, *J. Electroanal. Chem.*, 2003, **556**, 127-136.
24 M. L. Foresti, M. Innocenti, F. Loglio, L. Becucci and R. Guidelli, *J. Electroanal. Chem.*, 2010, **649**, 89-94.
25 B. M. Jović, V. D. Jović and D. M. Dražić, *J. Electroanal. Chem.*, 1995, **399**, 197-206.
26 K. R. Temsamani and K. Lu Cheng, *Sens. Actuators, B*, 2001, **76**, 551-555.
27 B. V. Andryushechkin, K. N. Eltsov and V. M. Shevlyuga, *Surf. Sci.*, 1999, **433–435**, 109-113.

28 K. J. Stevenson, X. Gao, D. W. Hatchett and H. S. White, *J. Electroanal. Chem.*, 1998, **447**, 43-51.
29 R. L. Wentworth, *The mechanism of the catalytic decomposition of hydrogen peroxide by silver*, M.I.T. Division of Industrial Cooperation, 1951.
30 F. T. Maggs and D. Sutton, *Trans. Faraday Soc.*, 1958, **54**, 1861-1870.
31 J. Bagg, *Aust. J. Chem.*, 1962, **15**, 201-210.
32 Q. Zhang, N. Li, J. Goebl, Z. Lu and Y. Yin, *J. Am. Chem. Soc.*, 2011, **133**, 18931-18939.
33 N. Li, Q. Zhang, S. Quinlivan, J. Goebl, Y. Gan and Y. Yin, *ChemPhysChem*, 2012, **13**, 2526-2530.
34 T. Parnklang, C. Lertvachirapaiboon, P. Pienpinijtham, K. Wongravee, C. Thammacharoen and S. Ekgasit, *RSC Adv.*, 2013, **3**, 12886-12894.
35 S. Nootchanat, C. Thammacharoen, B. Lohwongwatana and S. Ekgasit, *RSC Adv.*, 2013, **3**, 3707-3716.
36 H. Chen, F. Simon and A. Eychmüller, *J. Phys. Chem. C*, 2010, **114**, 4495-4501.
37 G. Cui, S. Qi, X. Wang, G. Tian, G. Sun, W. Liu, X. Yan, D. Wu, Z. Wu and L. Zhang, *J. Phys. Chem. B*, 2012, **116**, 12349-12356.
38 CRC Handbook of Chemistry and Physics, 90th edn (CD-ROM Version 2010), ed. D. R. Lide, CRC Press/Taylor and Francis, Boca Raton, Florida, 2010.
39 P. M. Ajayan and L. D. Marks, *Phys. Rev. Lett.*, 1988, **60**, 585-587.
40 R. Nasanen, *Acta Chem. Scand.*, 1947, **1**, 763-769.
41 C.-M. Ho, S. K.-W. Yau, C.-N. Lok, M.-H. So and C.-M. Che, *Chem. Asian. J.*, 2010, **5**, 285-293.
42 Y.-I. Lee, S. Kim, S.-B. Jung, N. V. Myung and Y.-H. Choa, *ACS Appl. Mater. Inter.*, 2013, **5**, 5908-5913.
43 F. R. Duke and T. W. Haas, *J. Phys. Chem.*, 1961, **65**, 304-306.
44 B. R. Panda and A. Chattopadhyay, *J. Nanosci. Nanotechnol.*, 2007, **7**, 1911-1915.
45 D. Jana and G. De, *J. Mater. Chem.*, 2011, **21**, 6072-6078.
46 X. Xia, J. Zeng, L. K. Oetjen, Q. Li and Y. Xia, *J. Am. Chem. Soc.*, 2011, **134**, 1793-1801.
47 Y. Sun, B. Mayers, T. Herricks and Y. Xia, *Nano Lett.*, 2003, **3**, 955-960.
48 J. C. Chuang, R. K. Haldar, J. J. Merianos, J. S. Shih, T. E. Smith, Strongly swellable, moderately crosslinked polyvinylpyrrolidone. WO1993021931 A1, Nov 11, 1993.
49 W. Kunda, Process for the production of elemental silver from silver chloride or silver sulphate. US4306902 A, Dec 22, 1981.
50 J. J. Merianos, Anhydrous complexes of PVP and hydrogen peroxide. US5008093 A, Apr 16, 1991.
51 E. F. Panarin, K. K. Kalninsh and D. V. Pestov, *Eur. Polym. J.*, 2001, **37**, 375-379.
52 H. Gatemala, C. Thammacharoen and S. Ekgasit, *CrystEngComm*, 2014, **16**, 6688-6696.
53 D. Aherne, D. M. Ledwith, M. Gara and J. M. Kelly, *Adv. Funct. Mater.*, 2008, **18**, 2005-2016.
54 J. Goebl, Q. Zhang, L. He and Y. Yin, *Angew. Chem. Int. Ed.*, 2012, **51**, 552-555.
55 M. Bowker, *J. Electron. Spectrosc. Relat. Phenom.*, 1986, **37**, 319-327.
56 D. Briggs, R. A. Marbrow and R. M. Lambert, *Chem. Phys. Lett.*, 1978, **53**, 462-464.
57 J. Sharma, P. DiBona and D. A. Wiegand, *Appl. Surf. Sci.*, 1982, **11–12**, 420-424.
58 C. A. Strydom, J. F. van Staden and H. J. Strydom, *J. Electroanal. Chem. Interfac.*, 1990, **277**, 165-177.
59 D. Hecht and H. H. Strehblow, *J. Electroanal. Chem.*, 1997, **440**, 211-217.
60 P. Prieto, V. Nistor, K. Nouneh, M. Oyama, M. Abd-Lefdil and R. Díaz, *Appl. Surf. Sci.*, 2012, **258**, 8807-8813.
61 A. Chen, K. Kamata, M. Nakagawa, T. Iyoda, Haiqiao and X. Li, *J. Phys. Chem. B*, 2005, **109**, 18283-18288.
62 P. S. Mdluli, N. M. Sosibo, P. N. Mashazi, T. Nyokong, R. T. Tshikhudo, A. Skepu and E. van der Lingen, *J. Mol. Struct.*, 2011, **1004**, 131-137.
63 M. Rycenga, C. M. Cobley, J. Zeng, W. Li, C. H. Moran, Q. Zhang, D. Qin and Y. Xia, *Chem. Rev.*, 2011, **111**, 3669-3712.
64 H. Wang, X. Qiao, J. Chen, X. Wang and S. Ding, *Mater. Chem. Phys.*, 2005, **94**, 449-453.
65 W.-T. Chen, C.-C. Ma, M.-H. Lee, Y.-C. Chu, L.-C. Tsai and C.-M. Shu, *App. Energy*., 2012, **100**, 187-192.
66 S. Aktas, *Hydrometallurgy*, 2010, **104**, 106-111.
67 C. W. Lee and K. W. Fung, *Resour. Recov. Conserv.*, 1981, **5**, 363-371.
68 A. V. Pethkar, S. K. Kulkarni and K. M. Paknikar, *Bioresour. Technol.*, 2001, **80**, 211-215.
69 N. Sathaiyan, V. Nandakumar and P. Ramachandran, *J. Power Sources*., 2006, **161**, 1463-1468.